Appendix. A

Seevinck's Companding Current-Mode Integrator

Driven by the need for achieving high-speed filtering function under low supply voltages, Seevinck proposed a novel companding current-mode integration scheme in 1990 [47]. Interesting, a linear integrator is designed out of nonlinear parts. The input current signal is compressed, and integrated by a capacitor to form a voltage, which when expanded forms an output linear current. Since both input and output signals are in the form of current, and signal compression and expansion are involved, the circuit was termed a companding current-mode integrator.

Although its development was totally independent of the log-domain filters (in fact, the log-domain principles did not catch much attention until it was resurrected by Frey [22] a few years later), the underlying principles are strikingly similar. Therefore, for completeness, this integrator is reviewed here. At the end, we will point out its relationship to log-domain integrators.

The block diagram of the integrator is shown in Figure A-l(a). A divider combines the input and output current and produces a compressed signal $I_o(I_{in}/I_{out})$, where I_o is a normalizing constant†. The current is integrated in capacitor *C,* and produces a voltage *v*, which is given by

†. As we will see shortly, this constant is physically realized by a dc bias current.

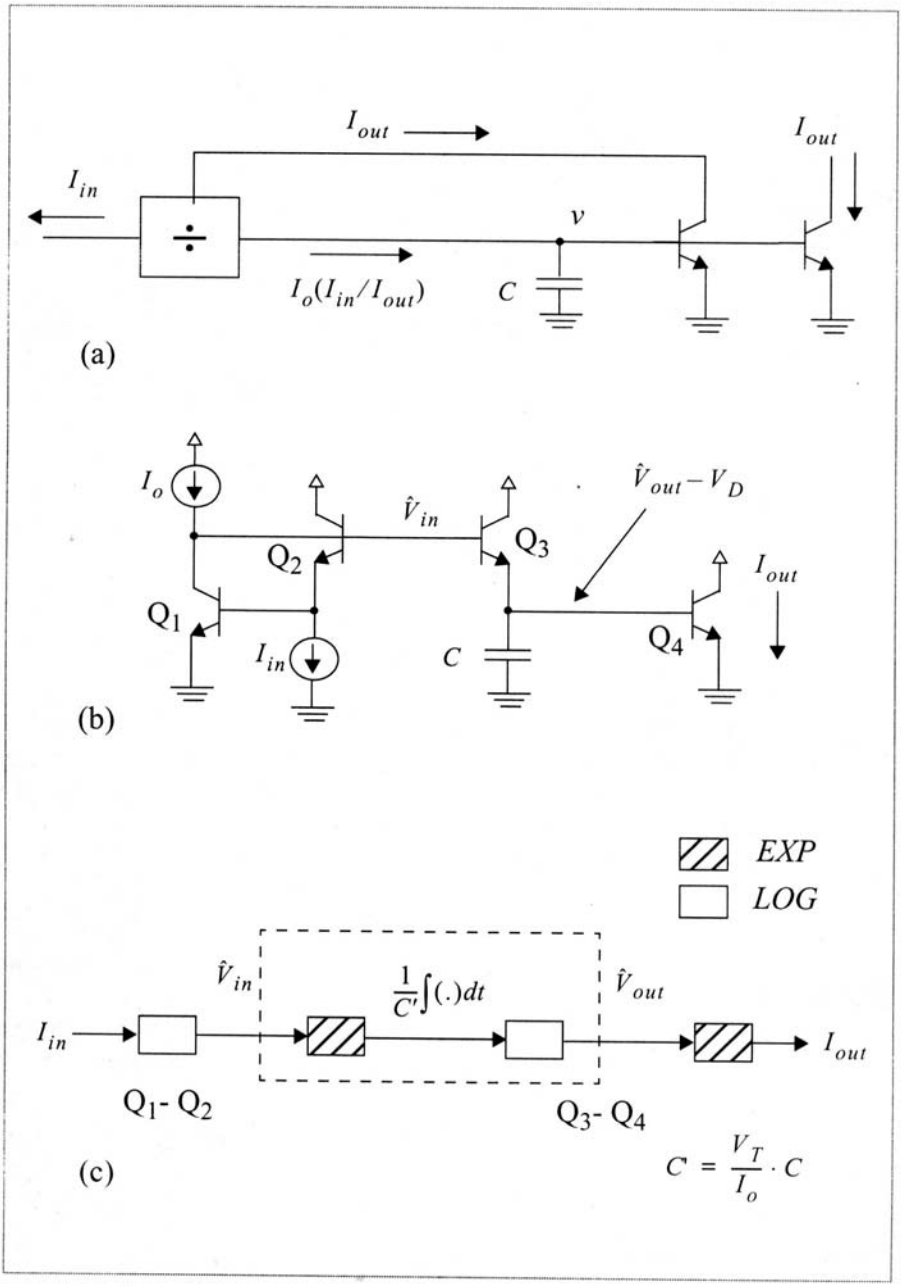

Figure A-1: Demonstration of companding current-mode integrator: (a) principle, (b) simplistic circuit implementation, and (c) log-domain SFG representation.

$$I_o \cdot \left(\frac{I_{in}}{I_{out}}\right) = C \cdot \frac{dv}{dt} \tag{A.1}$$

A bipolar transistor then serves as a transconductor to expand v into the current I_{out} with the familiar exponential relationship,

$$I_{out} = I_S e^{v/V_T} \tag{A.2}$$

Eliminate v by combining (A.1) and (A.2), we have

$$I_o \cdot \left(\frac{I_{in}}{I_{out}}\right) = C \cdot \frac{d}{dt}\left[V_T \cdot \ln\left(\frac{I_{out}}{I_S}\right)\right] \tag{A.3}$$

Integrating each side, and arrange, we arrive at

$$I_{out} = \frac{I_o}{V_T C} \cdot \int I_{in} dt \tag{A.4}$$

Although the intermediate steps involve nonlinear signal operations such as division and exponentiation, the input-output behavior is linear. Notice that the unity gain frequency is controllable through the constant I_o. Seeing that the currents in (A.1) are arranged in product pairs, by the translinear principle described in Chapter 1, the companding integrator can be realized by the simple circuit of Figure A-1(b)†.

Now, we would like to show how the integrator circuit can be understood in using the log-domain analysis presented in Chapter 2. To do so, define the log-domain signals as shown in Figure A-1(b), and a pair of complementary *LOG/EXP* operators as

$$LOG(X) = V_T \cdot \ln\left(\frac{I_o \cdot X}{I_S^2}\right) \qquad EXP(X) = \frac{I_S^2}{I_o} \cdot e^{X/V_T} \tag{A.5}$$

This then allows us to write the input log-domain voltage $\hat{V}_{in} = LOG(I_{in})$ generated by Q_1-Q_2 as

---

†. This circuit of Figure A-1(b) is not practical as it lacks a discharge path for the capacitor. However, it is sufficient to highlight the integrator concept without burdening the readers with non-essential details. For more complete and sophisticated implementations, such as the Class AB circuit, please refer to [47].

$$\begin{aligned}\hat{V}_{in} &= V_D + V_T \cdot \ln\left(\frac{I_{in}}{I_S}\right) \\ &= V_T \cdot \ln\left(\frac{I_o I_{in}}{I_S^2}\right)\end{aligned} \tag{A.6}$$

where V_D is the diode drop across the bipolar transistor Q_1 with dc bias current I_o. Notice that $\hat{V}_{in}$ is equal to $LOG(I_{in})$. Transistor Q_3 and the capacitor then perform integration, and produce a level-shifted log-domain output voltage, $\hat{V}_{out} - V_D$. The KCL equation at the capacitor node is found to be

$$I_S \cdot e^{\frac{\hat{V}_{in} - \hat{V}_{out} + V_D}{V_T}} = C \cdot \frac{d}{dt}(\hat{V}_{out} - V_D) \tag{A.7}$$

Multiply both sides by $e^{\hat{V}_{out}/V_T}$, and rewrite V_D in terms of the diode equation, we have

$$I_o \cdot e^{\frac{\hat{V}_{in}}{V_T}} = C \cdot e^{\frac{\hat{V}_{out}}{V_T}} \cdot \frac{d}{dt}(\hat{V}_{out}) \tag{A.8}$$

Apply the chain rule and re-arrange to obtain

$$\frac{I_S^2}{I_o} \cdot e^{\frac{\hat{V}_{in}}{V_T}} = \frac{CV_T}{I_o} \cdot \frac{d}{dt}\left(\frac{I_S^2}{I_o} \cdot e^{\frac{\hat{V}_{out}}{V_T}}\right) \tag{A.9}$$

In terms of the *LOG* operators, we arrive at a log-domain transfer function similar to the one in (2.5), given by

$$EXP(\hat{V}_{out}) = \frac{I_o}{CV_T} \cdot \int (EXP(\hat{V}_{in}))dt \tag{A.10}$$

Finally, transistor Q_4 acts as a exponential transconductor and converts the voltage $\hat{V}_{out} - V_D$ to a linear current I_{out}, so that

$$\begin{aligned} I_{out} &= I_S \cdot e^{\frac{\hat{V}_{out} - V_D}{V_T}} \\ &= \frac{I_S^2}{I_o} \cdot e^{\frac{\hat{V}_{out}}{V_T}} \\ &= EXP(\hat{V}_{out}) \end{aligned} \tag{A.11}$$

The log-domain SFG is represented in Figure A-l(c). In principle, the companding current-mode integrator is remarkably similar to those used in log-domain circuits. Although the *LOG* and *EXP* operators presented here are different from those in (2.4), this circuit will share many characteristics of the log-domain integrator presented previously.

Appendix. B

Multitone Testing Using *SPICE*

SPICE simulation is limited by its inability to perform AC analysis on non-linear circuits. This is due to the fact that when performing AC analysis, *SPICE* first solves for the DC operating point of the circuit, then determines linearized, small-signal models for all of the non-linear devices in the circuit. This is particularly relevant when simulating the log-domain filter since the exponential nature of the bipolar transistor is at the very heart of its operation.

The solution is to use a technique called *multitone testing* [71], [75]. Multitone testing involves applying a stimulus composed of one or more tones to the device under test and observing its spectral response. It is commonly used in the testing community and permits the simultaneous measurement of frequency response, total harmonic distortion (THD) and inter-modulation distortion (IMD), thereby reducing test time.

This appendix will show how SPICE transient analysis can be used to perform this kind of testing. The basic approach is as follows. First, SPICE is used to find the transient response of a circuit subjected to a multitone stimulus. Then the mathematical software package MATLAB finds the discrete Fourier transform of the transient output and plots it with respect to frequency.

B.1 Review of the Discrete Fourier Transform

In order to understand some of the constraints that will be imposed on the analysis, we begin with a review of the discrete Fourier transform (DFT) [76].

For every discrete-time sequence *x(n)* there exists a Fourier transform which is defined by:

$$X(\omega) = \sum_{-\infty}^{\infty} x(n) e^{-j\omega n} \tag{B.1}$$

Suppose we now limit the length of *x(n)* to *L* samples, such that:

$$x'(n) = \begin{cases} x(n) & 0 \le n \le L-1 \\ 0 & n > L-1 \end{cases} \tag{B.2}$$

The Fourier transform of this sequence will now be given by:

$$X(\omega) = \sum_{n=0}^{L-1} x'(n) e^{-j\omega n}$$

We now sample *X(ω)* at *N* equally spaced frequencies $\omega_k = \frac{2\pi k}{N}$, *k=0,1,...,N-1* and $N \ge L$, such that:

$$X(k) \equiv X\left(\frac{2\pi k}{N}\right) = \sum_{n=0}^{L-1} x'(n) e^{-j\frac{2\pi kn}{N}}, \quad k = 0, 1, 2, \ldots, N-1$$

which can be rewritten as:

$$X(k) = \sum_{n=0}^{N-1} x'(n) e^{(-j2\pi kn)/N}, \qquad k = 0, 1, 2, \ldots, N-1 \tag{B.3}$$

Equation (B.3) denotes the relationship for transforming a sequence $\{x'(n)\}$ of length $L \le N$ into a sequence of frequency samples $\{X(k)\}$ of length *N*, and is called the *discrete Fourier transform* (DFT). The relationship that allows us to recover the sequence $\{x'(n)\}$ from a set of frequency samples is called the inverse discrete Fourier transform (IDFT) and is given by:

$$x'(n) = \frac{1}{N} \cdot \sum_{k=0}^{N-1} X(k) e^{(j2\pi kn)/N}, \qquad n = 0, 1, 2, \ldots, N-1 \tag{B.4}$$

The DFT is usually computed using any of a number of efficient algorithms that are called Fast Fourier Transforms (FFT).

B.2 The *SPICE* File

The first step in multitone analysis is to use *SPICE* to find the transient response of a circuit stimulated by one or more sinusoidal tones. For those who are unfamiliar with transient analysis, *SPICE* finds the circuit solution at a set of discrete-time intervals. Consequently, the outcome of the analysis will be a sequence of discrete-time samples $\{x'(n)\}$ that can be used to compute the discrete Fourier transform as described in the previous section.

The *SPICE* file describes the different circuit components that make up the log-domain filter [77]. When preparing a *SPICE* file for multitone analysis, special care must be taken in two particular areas. First, the signal sources that make up the multitone input must be properly defined such that they have the right frequency, amplitude and phase. Each of these areas will be discussed at some length. Second, the transient analysis requests must be chosen correctly since the computation of the FFT depends on the proper transient output.

B.2.1 The Signal Sources

The circuit is to be stimulated by a set of sinusoidal current sources each operating at a different frequency. This section will outline some guidelines that govern the choice of frequency, amplitude and phase of the different tones in the multitone input.

B.2.1.1 Frequency

The choice of frequency for each different tone is important for two reasons:

1. The frequency of each input tone must correspond to one of the discrete frequency points in the DFT. This will ensure that every input tone completes an integral number of cycles over the total simulation time and thus prevents leakage and spreading effects.

2. The frequency of the different tones should not be multiples of one another. This will minimize the chance that their harmonics and intermodulation products coincide.

The choice of sampling frequency and of the unit test period (a concept to be defined next) will help us meet these constraints:

a) The unit test period

In order to minimize leakage effects when calculating the DFT of a multitone system, we must ensure that each sinusoid in the multitone input completes an integral number periods over the time of the analysis. The shortest time interval which allows this for all tones is called the *unit test period* (UTP). For example, the unit test period for an input composed of 2 kHz, 3 kHz and 5 kHz sine waves is 1 ms, as shown in Figure B-1. The reciprocal of the UTP is called the primitive frequency and corresponds to the greatest divisor of the input frequencies (1 kHz in our example). The value of the primitive frequency will help determine the sampling frequency.

b) The sampling frequency

Since we want each of the input frequencies to correspond to one of the discrete frequencies in the DFT, we let the sampling frequency be given by:

$$f_s = N \cdot f_p \tag{B.5}$$

where N = *Number of points in the DFT*
f_p = *Primitive frequency*

Figure B-2 shows the results of a 16 point DFT performed on a system composed of the three sine waves described in the previous section. Note that the sampling frequency is 16 kHz. Only the first eight samples are shown since the other eight are given by the mirror image of the first ones.

An additional problem that will affect the choice of the sampling frequency is aliasing. We know from the Nyquist Sampling Theory that in

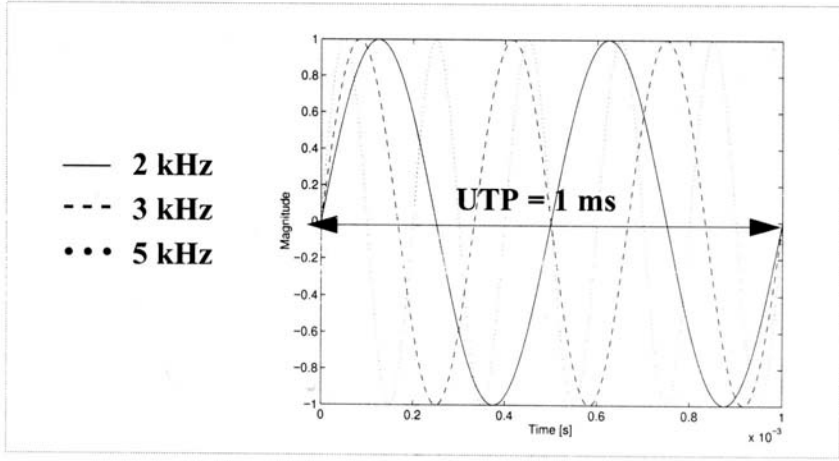

Figure B-1: Calculating the unit time period of a 3-tone input.

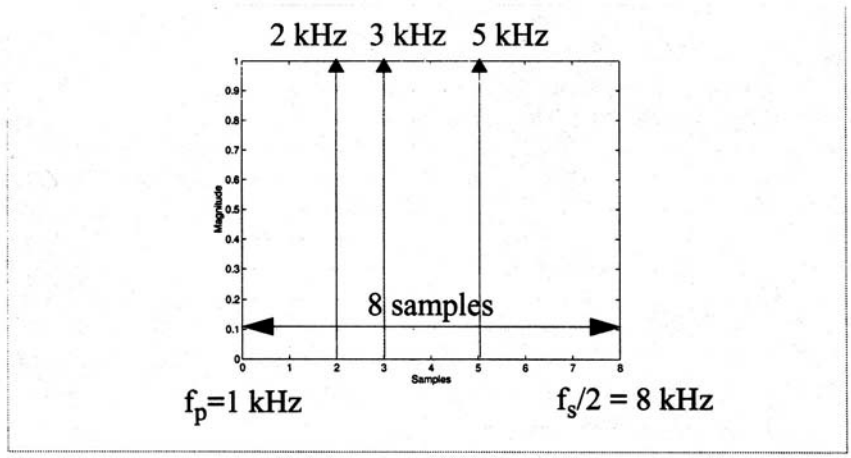

Figure B-2: Illustrating the relationship between the sampling frequency and other multitone parameters.

order to prevent aliasing, we must make sure that the highest frequency contained in the sampled signal is less than the Nyquist frequency, $f_s/2$. In other words, all of the input tones must be at frequencies less than $f_s/2$ Even with this precaution, we may get aliasing if any of the harmonics or the inter-modulation products are greater than the Nyquist frequency. In this case, some kind of anti-aliasing filter would be needed. Most of the analysis done is this work was done such that the cutoff frequency of the filter to be tested was much less than $f_s/2$. Therefore, the natural attenuation of the filter limits the effect of aliasing and eliminates the need for an anti-aliasing filter.

c) Frequency resolution

For a given sampling frequency, increasing the number of points in the DFT (*N*) will increase the frequency resolution of the spectral output. Changing *N* is analogous to controlling the resolution bandwidth on a spectrum analyzer. The drawback to choosing a large *N* is that the number of samples needed for the transient analysis is large and thus increases the simulation time. Usually, one attempts to find a balance between spectral resolution and run time. A second constraint on *N* is the type of FFT algorithm used. A radix-2 algorithm needs 2^N samples while a radix-3 algorithm needs 3^N samples and so on. In our case, the radix-2 algorithm was always used since it is generally faster. As a result, *N must always be a power of 2.*

d) Interference

Each tone must be placed at a frequency that will minimize the chance that its harmonics and intermodulation distortion terms fall in the same frequency bin. This is in general a very complicated process. Often one simply tries to use a scheme that forces any possible overlapping harmonics to be as high order as possible. There are a number of approaches that can be used:

Prime-Rich Signals

One strategy is to base the set of input frequencies exclusively on prime numbers. This ensures that none of the input frequencies are harmonic to one another and that no sum or difference products fall on a test frequency. Unfortunately, it does not prevent third and fifth order intermodulation interference.

An Iterative Scheme

Restricting the tones to prime numbers is a tedious process. Because of the large number of constraints which are placed on the multitone stimulus we eventually want to be able to automate the process by writing a computer program that will automatically give us the frequency and other parameters for each tone. As a result, a formula for deriving the frequency of each tone was borrowed from telecom CODEC applications. The frequency of each tone is computed as follows:

$$f_{tone_i} = \frac{M_i}{N} \cdot f_s \tag{B.6}$$

where:

$$f_s = sampling\ frequency$$

$$N = Number\ of\ points\ in\ the\ DFT$$

$$M_i = 9 + [i \times 16] \tag{B.7}$$

$$i = 0,1,2,\ldots\ as\ long\ as\ M_i < (N/2)$$

This method is more susceptible to interference between the harmonics of the different input tones than the prime-rich scheme was. For example, the frequency of the 16th harmonic of the first input tone will be the same as the frequency of the 16th tone; hence, they will interfere with one another. The advantage of this particular scheme is that it is easier to implement algorithmically. The designer must decide whether the added interference is worth the greater ease of design.

B.2.1.2 Phase

As the periods of each sinusoid in the multitone input are related to one another, the sinusoids will tend to peak at the same points in time. When many tones are used this could lead to clipping in the circuit. The solution is to assign a random phase shift to each different sinusoid. This is easily done since *SPICE* can accept a phase shift as one of the parameters of the input.

B.2.1.3 Amplitude

Even with phase shifting, the average power of the multitone signal will increase with the number of tones used. To prevent overdriving the circuit, the amplitude of each tone will be restricted to some reasonable value. Our strategy is to assign the amplitude of each sinusoid according to the following equation:

$$\text{RMS of single tone} = \text{Desired RMS of multitone} / \sqrt{K} \tag{B.8}$$

where K = the number of tones in the multitone signal. For a sinusoid,

$$\textit{Peak of single tone} = \textit{RMS of single tone} * \sqrt{2} \tag{B.9}$$

Therefore,

$$\textit{Peak of single tone} = \textit{Desired RMS of multitone} * \sqrt{\frac{2}{K}} \tag{B.10}$$

B.2.1.4 A Complete SPICE Current Source

A typical *SPICE* statement for one of the current sources in the multitone input is shown below:

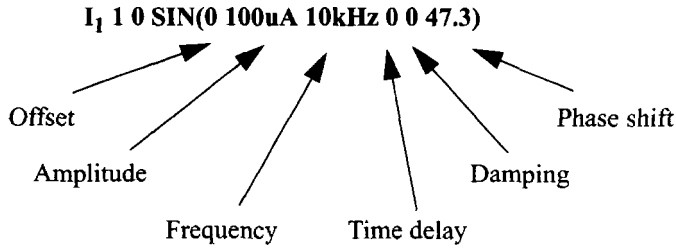

Some of these parameters are of no consequence in our analysis and hence have been set to zero.

B.2.2 Analysis Requests

SPICE is told what type of analysis to perform by a command called an *analysis request.* We wish to perform transient analysis such that we produce a sequence of discrete-time samples $\{x'(n)\}$ that represent the output current of the

log-domain filter. This sequence will then be used to compute its discrete Fourier transform

The *SPICE* request for transient analysis is done through the .TRAN command. A typical .TRAN statement is shown below:

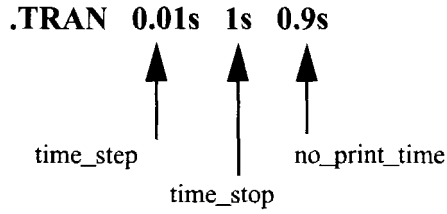

The three times are calculated as follows:

time_step: The step time is given by the sampling frequency.

$$time_{step} = \frac{1}{f_s} = T_s \tag{B.11}$$

time_stop: The stop time would normally be the time for one unit test period which is related to the sampling frequency by:

$$UTP = N \cdot T_s \tag{B.12}$$

However, we wish to allow the simulation to run long enough for the output to settle down [78]. Therefore, the total stop time is defined as:

$$time_{stop} = NP \cdot N \cdot T_s \tag{B.13}$$

where NP = *Number of periods needed for the simulation to settle down.*

no_print_time: This makes sure that only the last N points are printed, and is computed according to:

$$\text{no\_print\_time} = [(NP-1) \cdot N \cdot T_s] + T_s \tag{B.14}$$

We now have all the tools necessary to perform a spectral analysis of our circuit. The next section will show a simple example of how this would be done.

B.3 An Example using the Log-Domain Biquad

We wish to obtain the frequency response of the log-domain lowpass biquad (Figure 3-7) described in Chapter 3. As we have some flexibility in choosing the component values of the biquad, we will choose:

$$I_o = 100\ uA$$

$$C_1 = 8.2\ nF$$

$$C_2 = 2.2\ nF$$

which we know from theory should give us a cutoff frequency of:

$$f_c = 63.8\ kHz$$

The sampling criteria is chosen as follows:

$$f_s = 500\ kHz$$

$$N = 512\ points$$

$$Number\ of\ Tones = 16$$

$$Number\ of\ Periods\ (NP) = 100$$

A C program was written which accounts for all of the criteria outlined in the previous two sections. The multitone inputs and the transient analysis statement were generated automatically and are shown below:

```
*** Multitone Sources ***
Is1 1 0 SIN(100uA 80uA  8789.0625 0 0
184.9)
Is2 1 0 SIN(100uA 80uA  24414.0625 0 0
63.2)
Is3 1 0 SIN(100uA 80uA  40039.0625 0 0
111.1)
Is4 1 0 SIN(100uA 80uA  55664.0625 0 0
192.4)
Is5 1 0 SIN(100uA 80uA  71289.0625 0 0
341.1)
Is6 1 0 SIN(100uA 80uA  86914.0625 0 0
61.8)
Is7 1 0 SIN(100uA 80uA  102539.0625 0 0
252.8)
Is8 1 0 SIN(100uA 80uA  118164.0625 0 0
81.5)
Is9 1 0 SIN(100uA 80uA  133789.0625 0 0
178.1)
Is10 1 0 SIN(100uA 80uA  149414.0625 0 0
44.8)
Is11 1 0 SIN(100uA 80uA  165039.0625 0 0
30.2)
Is12 1 0 SIN(100uA 80uA  180664.0625 0 0
140.2)
Is13 1 0 SIN(100uA 80uA  196289.0625 0 0
99.8)
Is14 1 0 SIN(100uA 80uA  211914.0625 0 0
132.5)
Is15 1 0 SIN(100uA 80uA  227539.0625 0 0
354.0)
```

```
Is16 1 0 SIN(100uA 80uA  243164.0625 0 0
192.7}

*** Analysis Requests ***
.THAN 0.000002 0.1024 0.101378 0.000002
```

We then run *SPICE* and use *MATLAB* to calculate the FFT of the output. The result is plotted and is shown in Figure B-3.

The reader can clearly see the presence of the 16 tones of the multitone input. This allows us to verify the frequency response and measure the cutoff frequency, which is around 65 kHz, as expected. The smaller tones represent the many intermodulation products that occur when a multitone signal is applied to a circuit with non-linearity present in it. Overall, we can see how this offers an excellent alternative for finding frequency information about non-linear circuits. By varying the number of tones at the input we can get total harmonic distortion and intermodulation distortion results, as well as frequency response.

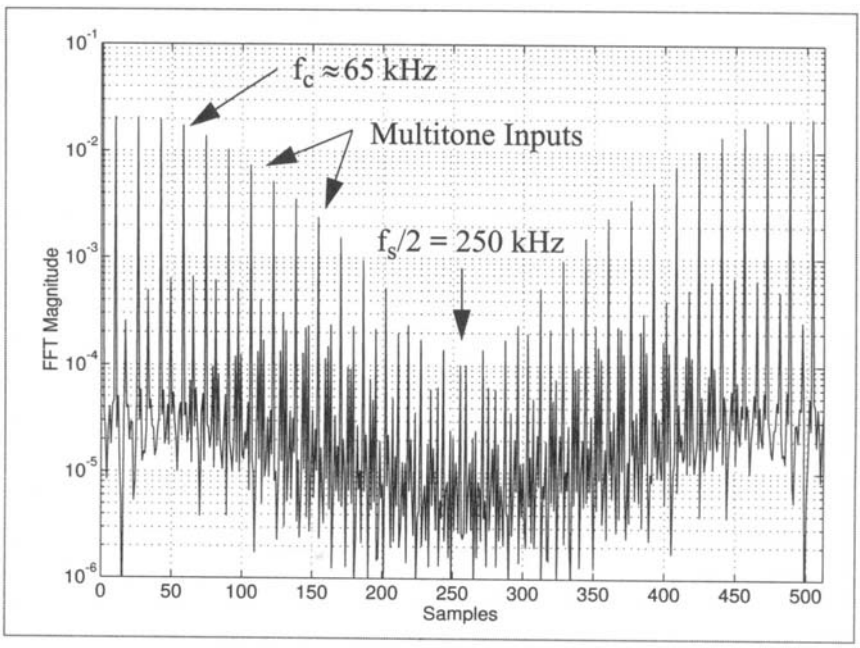

Figure B-3: FFT response of the log-domain biquad.

Appendix. C

Synthesis of High-Order Log-Domain Filters by a Cascade of Biquads

To illustrate the low-sensitivity of the ladder-based log-domain filter in Section 3.5 of Chapter 3, a seventh-order Chebyshev lowpass filter consisting of a cascade of biquads was used for comparison. In this appendix we shall describe the details of this filter.

A seventh-order filter consists of three second-order sections and one first-order section in cascade is shown in Figure C-1. The first three stages are similar to the lowpass biquad filter shown in Figure 3-7 without the output *EXP* stage. In addition, the input for each biquad is applied to the usually ground terminal of the *LOG* input stage. In this way, a natural *LOG-EXP* cancellation occurs between stages. The one-pole filter section is realized using the damped positive integrator shown in Figure 2-4 of Chapter 2. The overall input-output (I_{out}/I_{in}) linearity is maintained with the addition of an output *EXP* block.

For the Chebyshev filter approximation, a simple Matlab command [53] can be employed

```
[Z, P, K]= cheb1ap(N, Rp);
```

which returns the zeroes (`Z`), poles (`P`) and filter gain (`K`) when the filter order (`N`) and passband ripple (`Rp`, in dB) are specified. For a 7th-order filter, we can then group six

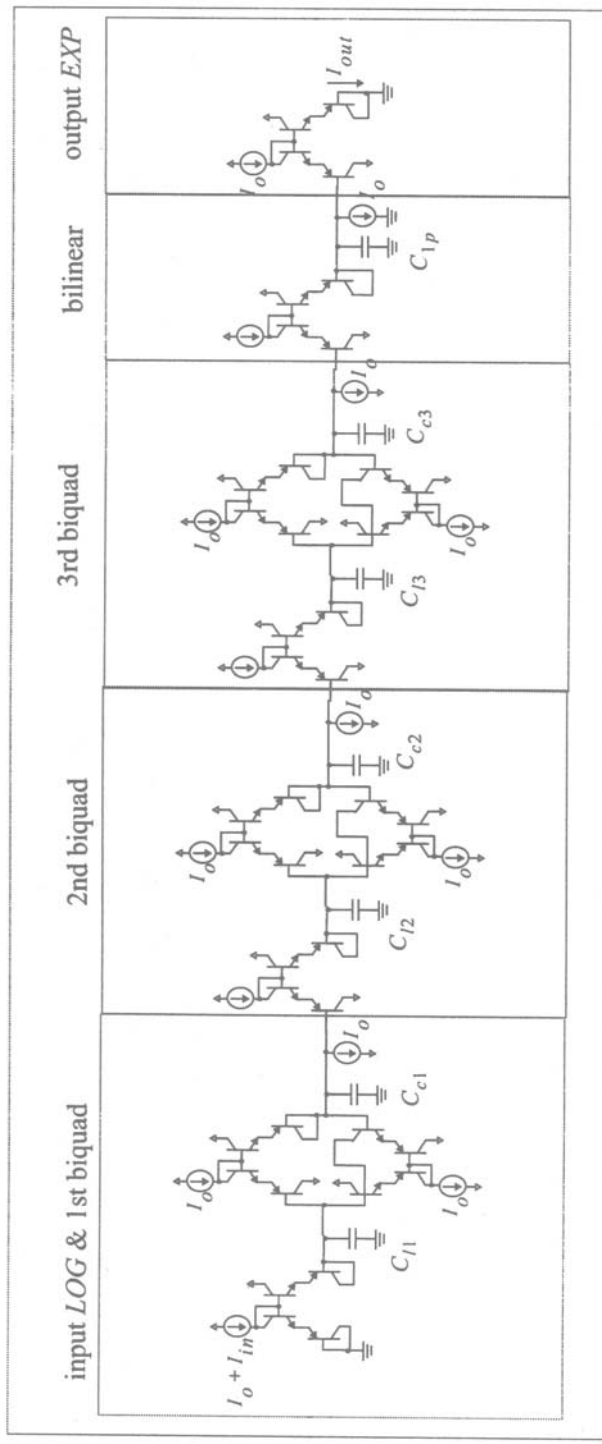

Figure C-1: 7th-order log-domain filter by biquad-cascade.

of the seven poles into three pairs. They will be realized by the three biquadratic filter sections. The remaining pole will be implemented by single first-order section. For a passband ripple of 1 dB and cutoff frequency of 1 MHz, the capacitor values of the log-domain filter were computed and are summarized in Table C-1.

1st biquad	C_{l1}	28.5155 pF	C_{c1}	3.3871 nF
2nd biquad	C_{l2}	0.1214 nF	C_{c2}	1.2089 nF
3rd biquad	C_{l3}	0.4973 nF	C_{c3}	0.8365 nF
bilinear	C_{1p}	1.5073 nF		

Table C-1: Capacitors of the 7th-order biquad-cascade log-domain filter.

Appendix. D

Derivation of Equation (5.16) - Compensation of Emitter Resistance, RE

In Chapter 5 we demonstrated a method in which to compensate for the effects of transistor nonzero emitter resistance RE. This involved tuning the log-domain integrator bias current from a nominal current level of I_o to a new value I_{comp} as described by (5.16). In this appendix, we shall derive this formula.

Assuming the bias current for the log-domain cell in Fig. 5-1 is changed from I_o to $k_c I_o$, we can write the RE-corrupted log-domain integrator expression as

$$k_c I_o e^{\frac{\hat{V}_{ip} - \hat{V}_o}{2V_T + 2R_E k_c I_o}} - k_c I_o e^{\frac{\hat{V}_{ip} - \hat{V}_o}{2V_T + 2R_E k_c I_o}} = C\frac{d}{dt}\hat{V}_o \qquad \text{(D.1)}$$

which is derived simply by replacing each occurrence of I_o in (5.8) by $k_c I_o$. Rearranging the expression, we get

$$k_c I_o e^{\frac{\hat{V}_{ip}}{2V_T + 2R_E k_c I_o}} - k_c I_o e^{\frac{\hat{V}_{ip}}{2V_T + 2R_E k_c I_o}} = C \cdot e^{\frac{\hat{V}_o}{2V_T + 2R_E k_c I_o}} \frac{d}{dt}\hat{V}_o \qquad \text{(D.2)}$$

which equals to

$$k_c\left(I_o e^{\frac{\hat{V}_{ip}}{2V_T+2R_Ek_cI_o}}-I_o\right)-k_c\left(I_o e^{\frac{\hat{V}_{in}}{2V_T+2R_Ek_cI_o}}-I_o\right) = \frac{2V_TC}{I_o}\cdot\left(\frac{2V_T+2R_Ek_cI_o}{2V_T}\right)\cdot\frac{d}{dt}\left(I_o e^{\frac{\hat{V}_o}{2V_T+2R_Ek_cI_o}}-I_o\right) \tag{D.3}$$

Defining the *EXP* and *LOG* complementary mappings as

$$\begin{aligned} EXP(x) &= I_o e^{\frac{x}{2V_T+2R_Ek_cI_o}}-I_o \\ LOG(x) &= (2V_T+2R_Ek_cI_o)\ln\left(\frac{I_o+x}{I_o}\right) \end{aligned} \tag{D.4}$$

we have

$$k_c\cdot EXP(\hat{V}_{ip})-k_c\cdot EXP(\hat{V}_{in}) = \frac{2V_TC}{I_o}\cdot\left(\frac{2V_T+2R_Ek_cI_o}{2V_T}\right)\cdot\frac{d}{dt}EXP(\hat{V}_o) \tag{D.5}$$

Rearranging, the log-domain integrator equation becomes

$$EXP(\hat{V}_o) = \left(\frac{V_Tk_c}{V_T+R_Ek_cI_o}\right)\cdot\frac{I_o}{2V_TC}\cdot\int\{EXP(\hat{V}_{ip})-EXP(\hat{V}_{in})\}dt \tag{D.6}$$

Comparing (D.6) and the ideal integration function (2.5), the effects of RE can be eliminated by setting the bracketed multiplicative factor to unity. Therefore, by setting

$$\frac{V_Tk_c}{V_T+R_Ek_cI_o} = 1 \tag{D.7}$$

the expression for k_c is found to be

$$k_c = \frac{V_T}{V_T-R_EI_o} \tag{D.8}$$

In summary, we can compensate for the RE nonideality by tuning I_o to k_cI_o where k_c is given by (D.8). This is the result shown in equation (5.16).

Appendix. E

Goodness of Fit Test

We have assumed that deviations of the log-domain filter due to area mismatches are normally distributed. Based on this assumption, confidence intervals of the performance criteria are derived for any given σ_X^2 (variance of the I_S) in Section 5.4.1. Here we will inquire how good the filter deviations approximate normal distribution.

From the Monte-Carlo simulation, 1000 observations of the filter deviations are generated for $\sigma_X^2 = 10^{-4}$, 10^{-3} and 10^{-2}. The *goodness-of-fit* test is applied to determine whether that set of data may be looked upon as a random sample from a population having a normal distribution. Assuming the data has a normal distribution with an estimated mean and variance, the statistic

$$\chi^2 = \sum_{i=1}^{m} \frac{(f_i - e_i)^2}{e_i} \qquad \text{where } m = \text{number of partitions}, \; f_i = \text{observed frequency in each partition}, \; e_i = \text{expected frequency in each partition} \tag{E.1}$$

should have a chi-square distribution with twenty-two degrees of freedom (i.e., m=25 and two estimated parameters in our assumed distribution) [62]. If the calculated χ^2 has low probability of occurrence, it implies the assumption of normal distribution is

not appropriate. As is common statistical practice, a probability of 0.05 is considered "low".

Applying the above test to our simulated data set in Section 5.4.1, the results are tabulated in Table E-1.

	Probability of the calculated χ^2		
σ_X^2	f_{oa}/f_o	Q_a/Q	K
1e-4	0.316	0.297	0.903
1e-3	0.724	0.762	0.196
1e-2	0.194	0.106	< 0.0001

Table E-1: Goodness-of-fit test on the simulated data shown in Section 5.4.1.

As displayed above, most of the probabilities take on values much higher than 0.05, showing that the normal-distribution-fit is very good and valid. Only when σ_X^2 becomes large (i.e., the variance of the transistor area is large), the normal distribution assumption becomes marginal and unacceptable.

References

[1] Y. P. Tsividis and J. O. Voorman, Eds., *Integrated Continuous-Time Filters*, Piscataway, NJ: IEEE Press, 1993.

[2] A. S. Sedra and K. C. Smith, *Microelectronics Circuits, 3rd Edition*, Florida, USA: Saunders College Publishing.

[3] A. Sedra and P. Brackett, *Filter Theory and Design: Active and Passive*, Portland, OR: Matrix Publishers Inc., 1978.

[4] S. Sakurai, M. Ismail, J. Michael, E. Sanchez-Sinencio and R. Brannen, "A MOS-C variable equalizer with simple on-chip automatic tuning," *IEEE J. of Solid-State Circuits*, vol. 27, no. 6, pp. 927-034, June 1992.

[5] J. van der Plaus, "MOSFET-C filter with low excess noise and accurate automatic tuning," *IEEE J. of Solid-State Circuits*, vol. 26, no. 7, pp. 922-929, July 1991.

[6] M. Banu and Y. P. Tsividis, "An elliptic continuous-time CMOS filter with on-chip automatic tuning," *IEEE J. of Solid-State Circuits*, vol. 20, no. 6, pp. 1114-1121, Dec. 1985.

[7] U. Moon and B. Song, "A low-distortion 22 kHz 5th-order Bessel filter," *IEEE Solid-State Circuits Conf., Dig. Tech. Papers*, vol. 36, pp. 110-111, Feb. 1993.

[8] A. B. Grebene, *Bipolar and MOS Analog Integrated Circuit Design*, New York, NY: John Wiley and Sons, 1984.

[9] W. M. Snelgrove and A. Shoval, "A balanced 0.9 μm CMOS transconductance-C filter tunable over the VHF range," *IEEE J. of Solid-Stale Circuits*, vol. 27, no. 3, pp. 314-323, March 1992.

[10] B. Nauta, "A CMOS transconductance-C filter technique for very high frequencies," *IEEE J. of Solid-State Circuits*, vol. 27, no. 2, pp. 142-153, Feb. 1992.

[11] M. I. Ali, M. Howe, E. Sanchez-Sinencio and J. Ramirez-Anulo, "A BiCMOS low distortion tunable OTA for continuous-time filters", *IEEE Trans. on Circuits and Systems I*, vol. 40, no. 1, pp. 43-49, Jan. 1993.

[12] J. Silva-Martinez, M. Steyaert and W. Sansen, "A large-signal very low-distortion transconductance for high-frequency continuous-time filters," *IEEE J. of Solid-State Circuits*, vol. 26. pp. 946-955, July 1991.

[13] S. D. Willingham and K. W. Martin, "A BiCMOS low-distortion 8 MHz lowpass filter, *IEEE Solid-State Circuits Conf., Dig. Tech. Papers*, vol. 36, pp. 114-115, Feb. 1993.

[14] R. Schaumann and M. A Tan, "The problem of on-chip automatic tuning in continuous-time integrated filters," *Proc. IEEE Int. Symp. on Circuits and Systems*, pp. 106-109, Feb. 1989.

[15] K. A. Kozma, D. A. Johns and A. S. Sedra, "Tuning of continuous-time filters in the presence of parasitic poles," *IEEE Trans. on Circuits and Systems I*, vol. 40, no. 1, pp. 13-20, Jan. 1993.

[16] B. Gilbert, "Current mode circuits from a translinear viewpoint: a tutorial," *Analog IC Design: The Current-Mode Approach*, C. Toumazou. F. Lidgey, and D. Haigh (eds.), IEE Circuits and Systems Series, vol. 2. Peter Perigrious Press, pp. 11-92, 1990.

[17] D. Frey, "Log-domain filtering for RF applications," *IEEE J. of Solid-State Circuits*, vol. 31, no. 10, pp. 1468-1475, Oct. 1996.

[18] M. El-Gamal, V. Leung and G. W. Roberts, "Balanced log-domain filters for VHF applications," *Proc. IEEE Int. Symp. on Circuits & Systems*, pp. 493-496, June 1997.

[19] F.Yang, C. Enz and G. van Ruymbeke, "Design of low-power and low-voltage log-domain filters," *Proc. IEEE Int. Symp. on Circuits & Systems*, pp. 117-120, May 1996.

[20] Y. Tsividis, "Externally linear, time-invariant systems and their application to companding signal processors" *IEEE Trans. on Circuits & Systems II*, vol. 44, no. 2, pp. 65-85, Feb. 1997.

[21] R. W. Adams, "Filtering in the log-domain," *Preprint #1470 presented at the 63rd AES Conference*, New York, NY, May 1979.

[22] D. Frey, "Log-domain filtering: an approach to current mode filtering," *IEE Proceedings-G*, vol. 140, no. 6, pp. 406-416, Dec. 1993.

[23] D. Frey, "A general class of current mode filters," *Proc. IEEE Int. Symp. on Circuits & Systems*, pp. 1435-1438, May 1993.

[24] D. Frey, "Current mode class AB second order filter," Electronics Letters, vol. 30, no. 3, pp. 205-206, Feb. 1994.

[25] D. Frey, "A 3.3 Volt electronically tunable active filter usable to beyond 1 GHz," *Proc. IEEE Int. Symp. on Circuits & Systems*, pp. 493-496, May-June 1994.

[26] D. Frey, "Exponential state space filters: A generic current mode design strategy," *IEEE Trans. Circuits and Systems I*, vol. 43, no. 1 pp. 34-42, Jan. 1996.

[27] D. Frey, "Log filtering using gyrators", Electronics Letters, vol. 32, no. 1, pp. 26-28, Jan. 1996.

[28] D. Frey, "An adaptive analog notch filter using log filtering," *Proc. IEEE Int. Symp. on Circuits & Systems*, pp. 297-300, May 1996.

[29] D. Perry and G. W. Roberts, "Log-domain filters based on LC ladder synthesis," *Proc. IEEE Int. Symp. on Circuits & Systems*, pp. 311-314, May 1995.

[30] D. Perry and G. W. Roberts, "Design of log-domain filters based on the operational simulation of LC ladders," *IEEE Trans. on Circuits & Systems II*, vol. 43, no. 11, pp. 763-773, Nov. 1996.

[31] M. El-Gamal and G. W. Roberts, "LC ladder-based synthesis of log-domain bandpass filters," *Proc. IEEE Int. Symp. Circuits & Systems*, pp. 105-108, June 1997.

[32] A. Hematy and G. Roberts, "A fully-programmable analog log-domain filter circuit," *Proc. 2nd IEEE-CAS Region 8 Workshop on Analog and Mixed IC Design*, Baveno, Italy, Sep. 1997.

[33] A. Hematy and G. Roberts, "A fully-programmable analog log-domain filter circuit," *Proc. IEEE Int. Symp. of Circuits & Systems*, pp. 309-312, May 1998.

[34] B. Gilbert, "Translinear circuits: a proposed classification," *Electron. Lett.*, vol. 11, no. 1, pp. 14-16, Jan. 1975.

[35] B. Gilbert, "A new wideband amplifier technique," *IEEE J. of Solid-State Circuits*, SC-3(4), pp. 355-365, 1968.

[36] B. Gilbert, "A precise four-quadrant multiplier with sub-nanosecond response," *IEEE J. of Solid-State Circuits*, SC-3(4), pp. 365-373, 1968.

[37] B. Gilbert, "Translinear circuits- 25 years on," Part I-III, *Electronics Engineering*, Aug.- Oct., 1993.

[38] B. Gilbert, "Translinear circuits: an historical overview," *Analog Integrated Circuits and Signal Processing*, vol. 9, n. 2, pp. 95-118, March, 1996.

[39] Members of the Technical Staff of Bell Telephone Laboratories, *Transmission Systems for Communications*, Bell Telephone Laboratories, Inc., 5th ed., 1982.

[40] Y. Tsividis, "Developments in integrated continuous-time filters," *Analog Circuit Design: Low-Power Low-Voltage, Integrated Filters and Smart Power*, R. J. van de Plassche, W. M. C. Sansen and J. H. Huijsing (eds.), pp. 129-148, Kluwer Academic Publishers, 1995.

[41] E. M. Drakakis, A. J. Payne, and C. Toumazou, "Log-domain filters, translinear circuits, and the Bernoulli cell," *Proc. IEEE Int. Symp. Circuits & Systems*, pp. 501-504, June 1997.

[42] M. N. El-Gamal and G. W. Roberts, "Very high-frequency log-domain bandpass filters," *IEEE Trans. on Circuits and Systems II*, vol. 45, no. 9, pp. 1188-1198, Sept. 1998.

[43] M. Punzenberger and C. Enz, "A new 1.2V BiCMOS log-domain integrator for companding current-mode filters," *Proc. IEEE Int. Symp. Circuits & Systems*, pp. 125-128, May 1996.

[44] M. Punzenberger and C. Enz, "A compact low-power BiCMOS log-domain filter," *IEEE J. of Solid State Circuits*, vol. 33, no. 7, pp. 1123-1129, July 1998.

[45] M. Punzenberger and C. Enz, "A 1.2-V low-power BiCMOS class AB log-domain filter," *IEEE. J. Solid State Circuits*, vol. 32, no. 12, Dec. 1997.

[46] M. N. El-Gamal and G. W. Roberts, "A new 1.2 V npn-only log-domain integrator," *Proc. Int. Symp. Circuits & Systems*, pp. II-681 -II-684, June 1999.

[47] E. Seevinck, "Companding current-mode integrator: a new circuit principle for continuous-time monolithic filters," *Electronics Letters*, vol. 26, no. 24, pp. 2046-2047, Nov. 1990.

[48] M. Van Valkenburg, *Analog Filter Design*, New York, NY:, Holt, Rinehart and Winston, 1982.

[49] W. Snelgrove and A. Sedra, *FILTOR2- A Computer Aided Filter Design Package*, Champagne, Ill.: Matrix Publishers.

[50] C. Ouslis, W. M. Snelgrove and A. S. Sedra, "A filter designer's filter design aid: filtorX," *Proc. IEEE Int. Symp. on Circuits & Systems*, pp. 376-379, 1991.

[51] J. Vlach and K. Singhal, *Computer Methods for Circuit Analysis and Design*, New York, NY: Van Nostrand Reinhold, 1983.

[52] Gennum Corporation, *Gennum Data Book*, 1995.

[53] The MathWorks Inc., *MATLAB Reference Guide*, 1995.

[54] W. M. Snelgrove and A. S. Sedra, "Synthesis and analysis of state-space active filters using intermediate transfer functions," *IEEE Trans. on Circuits and Systems*, vol. CAS-33, pp. 287-301, Mar. 1986.

[55] H. J. Orchard, "Inductorless filters," *Electronics Letters*, vol 2, pp. 224-225, June 1966.

[56] H. J. Orchard, G. C. Temes, and T. Cataltyepe, "Sensitivity formulas for terminated lossless two-ports," *IEEE Trans. on Circuits and Systems*, vol. CAS-32, pp. 459-466, May 1985.

[57] D. A. Johns, A. S. Sedra, "State-space Simulation of LC Ladder Filter," *IEEE Trans. on Circuits and Systems*, vol. CAS-34, pp. 986-988, August 1987.

[58] V. Leung, M. El-Gamal and G. Roberts, "Effects of transistor nonidealities on log-domain filters," *Proc. IEEE Int. Symp. on Circuits & Systems*, pp. 109-112, June 1997.

[59] V. Leung and G. W. Roberts, "Analysis and Compensation of Log-Domain Filter Response Deviations due to Transistor Nonidealities," *Analog Integrated Circuits and Signal Processing*, (in press).

[60] E. Seevinck, *Analysis and Synthesis of Translinear Integrated Circuits*, Studies in Electrical and Electronic Engineering, Elsevier, 1988.

[61] M. Ismail and T. Fiez (eds.), *Analog VLSI: Signal and Information Processing*, pp. 618-619, McGraw-Hill, 1994.

[62] J. E. Freund and R. E. Walpole, *Mathematical Statistics (4th ed.)*, Englewood Cliffs, NJ: Prentice-Hall, 1987.

[63] G. W. Roberts, "Gm-C integrator: magnitude and phase errors", *Analog Signal Processing Course Notes*, McGill University, 1998.

[64] G. Temes and H. Orchard, "First order sensitivity and worst case analysis of doubly terminated reactance two-ports," *IEEE Trans. on Circuit Theory*, vol. CT-20, pp. 567-571, Sept. 1973.

[65] M. Blostein, "Sensitivity analysis of parasitic effects in resistance terminated LC filters," *IEEE Trans. on Circuit Theory*, vol. CT-14, pp. 21-25, March 1967.

[66] D. Perry, "The design of log-domain filters based on the operational simulation of LC ladders," *Master's Dissertation*, McGill University, Montreal, Canada, 1995.

[67] R. A. Witte, *Spectrum and Network Measurements*, NJ: Prentice-Hall, 1991.

[68] R. Caprio, "Precision differential voltage-current converter," *Electronics. Letters*, vol. 9, no. 6, pp. 147-148, Mar. 1973.

[69] J. F. Jensen, G. Raghavan, A. E. Cosand, and R. H. Walden, "A 3.2GHz second-order delta-sigma modulator implemented in InP HBT technology," *IEEE J. Solid-State Circuits*, vol. 30, pp. 1119-1127, Oct. 1995.

[70] M. El-Gamel, "Generalized log-domain integrator structure & its application to the synthesis of high-frequency and low-voltage log-domain filters," *Ph.D.'s Dissertation*, McGill University, 1998.

[71] G. W. Roberts, "Calculating distortion levels in sampled-data circuits using SPICE," *IEEE Int. Symp. on Circuits and Systems*, Seattle, Washington, vol. 3, pp. 2059-2062, May 1995.

[72] P. R. Belanger, *Control Engineering: A Modern Approach*, Oxford University Press, 1995.

[73] Robert M. Fox; "Design-oriented analysis of log-domain circuits," *IEEE Trans. Circuit Syst. II*, vol. 45, pp. 918-921, July 1998.

[74] A. Hematy, "Digitally programmable analog log-domain filters," *M. Eng.'s Dissertation*, McGill University, November 1998.

[75] M. Mahoney, *DSP-Based Testing of Analog and Mixed-Signal Circuits*, New York, NY: IEEE Computer Society Press, 1987.

[76] J. G. Proakis and D. G. Manolakis, *Digital Signal Processing*, New York, NY: MacMillan Publishing Co., 1992.

[77] G. W. Roberts and A. S. Sedra, *SPICE, 2nd Edition*, Oxford University Press, 1992.

[78] P. Crawley and G. W. Roberts, "Predicting harmonic distortion in switched-current memory circuits", *IEEE Trans. on Circuits and Systems -I: Fundamental Theory and Applications*, Vol. 41, pp. 73-86, Feb. 1994.

Index